Electrochemistry and Electrogenerated Chemiluminescence of a Novel Donor−Acceptor FPhSPFN Red Fluorophore

Mei Shen,[†] Joaquín Rodríguez-López,[†] Yi-Ting Lee,[‡,§] Chin-Ti Chen,[§] Fu-Ren F. Fan,[†] and Allen J. Bard*[,†]

Center for Electrochemistry, Department of Chemistry and Biochemistry, University of Texas at Austin, 1 University Station, A5300 Austin, Texas 78712-0165, Department of Chemistry, National Central University, Jhongli, Taiwan 320, Republic of China, and Institute of Chemistry, Academia Sinica, Taipei, Taiwan 11529, Republic of China

Received: December 2, 2009; Revised Manuscript Received: April 15, 2010

We report here the electrogenerated chemiluminescence (ECL) of a red fluorophore diphenylaminospirobifluorenylfumaronitrile (FPhSPFN). FPhSPFN contains two diphenylamino groups as strong electron donors at the ends linked through a nonplanar bulky spirobifluorene linker to a common fumaronitrile group as a strong electron acceptor. The cyclic voltammetry of this compound shows two one-electron transfer reduction waves and one single overall two-electron oxidation wave consisting of closely spaced waves with a peak separation of 63 mV. Chronoamperometry with an ultramicroelectrode (UME) confirmed that each reduction wave involves a 1e transfer and that the oxidation wave contains an overall 2e transfer. The first reduction wave is Nernstian, $E^{o}_{1,red} = -1.09$ V versus SCE, and the second reduction wave, $E^{o}_{2,red} = -1.50$ V versus SCE, produces a film on the electrode. By comparison to a digital simulation, the oxidation is assigned to two reversible, closely spaced, one-electron processes for oxidation with $E^{o}_{1,ox} = 1.05$ V and $E^{o}_{2,ox} = 1.11$ V versus SCE. A large wavelength shift (∼35 nm) was observed in ECL as compared to photoluminescence (PL). The ECL spectrum showed a maximum emission at 708 nm with a red-shifted shoulder at around 750 nm. ECL was studied in mixtures of benzene/acetonitrile at different composition ratios; an increase in the ratio of the ECL intensity of the shoulder with respect to the main peak emission was observed with increasing solvent polarity. ECL generated with BPO as a coreactant also showed the red-shifted shoulder at the same ratio as that with annihilation.

Introduction

We report here an electrochemical and spectroscopic study of a novel donor−acceptor-based molecule, that is, diphenylaminospirobifluorenylfumaronitrile (FPhSPFN) red fluorophore, as well as its electrogenerated chemiluminescence (ECL) that results from the annihilation reaction between the radical anions and radical cations generated during electrochemical reduction and oxidation.

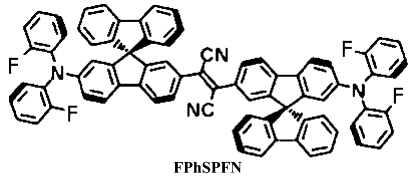

FPhSPFN

Annihilation ECL includes the process of generation of an excited singlet state (S route) through the electron transfer between electrochemically generated species and the following emission of light.[1,2] This process can be represented in a general way as shown in Scheme 1.

Scheme 1

$$A + e^- \rightarrow A^{-\bullet} \quad \text{(reduction at electrode)} \quad (1)$$

$$D - e^- \rightarrow D^{+\bullet} \quad \text{(oxidation at electrode)} \quad (2)$$

$$A^{-\bullet} + D^{+\bullet} \rightarrow {}^1A^* + D \quad \text{(excited singlet state formation)} \quad (3)$$

$$^1A^* \rightarrow A + h\nu \quad \text{(light emission)} \quad (4)$$

where A and D are electroactive species and denote the acceptor and donor, respectively. A and D can belong to different molecules as in mixed ECL systems but often represent energy levels (i.e., LUMO and HOMO) within the same molecule that are accessible electrochemically to generate a radical cation and a radical anion. ECL can be obtained in this way from species such as aromatic heterocycles or hydrocarbons.[3] A typical case is the efficient ECL emitter 9,10-diphenylanthracene (DPA).[4,5]

The excited singlet state is not always formed directly during the annihilation reaction. When the energy of the annihilation reaction is significantly smaller than the energy of the emitting singlet state, a triplet excited state could be formed. In this case, the process of triplet−triplet annihilation (T route) outlined in Scheme 2 follows to form the emitting singlet.

* To whom correspondence should be addressed. E-mail: ajbard@mail.utexas.edu.
[†] University of Texas at Austin.
[‡] National Central University.
[§] Academia Sinica.

10.1021/jp911451v
Published on Web 05/06/2010

Scheme 2

$$A^{-\bullet} + D^{+\bullet} \rightarrow {}^3A^* + D \quad \text{(excited triplet state formation)} \tag{5}$$

$${}^3A^* + {}^3A^* \rightarrow {}^1A^* + A \quad \text{(triplet−triplet annihilation)} \tag{6}$$

Except for notable exceptions, as proposed for rubrene,[6] the increase in the complexity of this mechanism is accompanied by a significant decrease in the ECL intensity. Coreactants are also used in ECL studies when one of the generated radical species is unstable or cannot be generated within the solvent window.[1,2] In the case of benzoyl peroxide (BPO), which will be used in the present study as a coreactant, a simplified mechanism follows in Scheme 3[7]

Scheme 3

$$BPO + e^- \rightarrow BPO^{-\bullet} \tag{7}$$

$$BPO^{-\bullet} \rightarrow C_6H_5CO_2^- + C_6H_5CO_2^{\bullet} \tag{8}$$

$$C_6H_5CO_2^{\bullet} + A^{-\bullet} \rightarrow C_6H_5CO_2^- + {}^1A^* \tag{9}$$

Notice that in both Schemes 1 and 2, the mechanism through which the excited state is formed involves an annihilation reaction between the molecules under study that may give rise to the formation of excimers; the coreactant scheme typically gives rise to emissive states devoid of this particular complication and as such has been used to distinguish spectral differences between ECL and PL.[7,8] D and A in Scheme 1 can also be different moieties within the same molecule, as in a donor and acceptor organic molecules. Recent ECL studies with these donor−acceptor-based molecules include the cases in which the donor and acceptor are either directly covalently connected[9−11] or connected through a linker.[12] The first case can be represented as D−A and the second case as D−X−A, where X is the linker. A number of donor−acceptor molecules have been the target of ECL studies, most commonly in the case of metal complexes,[13] for example, the widely used $Ru(bpy)_3^{2+}$,[14] in which electrochemical oxidation occurs in the Ru(II) center while reductions occur in the bipyridine ligands, the emitting state being a metal to ligand charge-transfer (MLCT) state.[15]

In FPhSPFN, the fumaronitrile moiety is a good electron acceptor (A),[16] and triphenylamine-based molecules are good electron donors (D).[11,17−19] Because of its structural rigidity, spirobifluorene has been used extensively in molecular design as a linker.[20−22] Here, we report the electrochemistry and ECL of FPhSPFN, where a fumaronitrile group is A and two substituted diphenylamines are D, linked through a spirobifluorene linker. FPhSPFN is a molecule designed for use in organic light-emitting devices (OLED). Several compounds used in OLEDs have been employed in ECL studies because they show good stability and high fluorescent efficiencies as both solids and solutions.[23−25] We have previously studied the ECL of fluorene-based OLED molecules that emit in the blue region.[26] Here, we examine the ECL of an OLED molecule that emits in the red region and exhibits a high solid-state fluorescence quantum yield (46% at 646 nm).[27]

Experimental Section

Materials. Anhydrous acetonitrile (MeCN) and benzene (PhH) were obtained from Aldrich (St. Louis, MO) and transferred directly into a helium atmosphere drybox (Vacuum Atmospheres Corp., Hawthorne, CA) without further purification. Electrochemical-grade tetra-*n*-butylammonium hexafluorophosphate ($TBAPF_6$) was obtained from Fluka and used as received. Benzoyl peroxide (BPO) was from Aldrich and was used as received. FPhSPFN was synthesized according to the literature procedure.[27]

Characterization. The same electrochemical cell was used for both cyclic voltammetry and ECL experiments; it consisted of a coiled Pt wire (0.5 mm in diameter) as a counter electrode, a Ag wire (0.5 mm in diameter) as a quasi-reference electrode, and a Pt disk inlaid in glass bent at a 90° angle (for the disk to face the photon detector) as a working electrode. The area of the Pt disk electrode was 0.019 cm^2 unless specifically noted. After each experiment, the potential of the Ag wire was calibrated with ferrocene (taken as 0.342 V versus SCE).[20] Before each experiment, the working electrode was polished on a felt pad with 0.3 μm alumina (Buehler, Ltd., Lake Bluff, IL) and sonicated in Milli-Q deionized water and then in ethanol. The counter and reference electrodes were cleaned by rinsing and sonicating in acetone, water, and ethanol. Finally, all of the electrodes were rinsed with acetone, dried in the oven, and transferred into the drybox. For chronoamperometry experiments, a 25 μm (in diameter) gold UME was used as a working electrode. The cleaning of the UME followed the same procedure as the cleaning of the macro working electrode.

Solutions for electrochemical measurements consisted of 0.5 mM FPhSPFN in a 2.33:1 (by volume) MeCN/PhH mixture (unless specifically indicated) as the solvent and 0.1 M $TBAPF_6$ as the supporting electrolyte. All solutions were prepared inside of the drybox. For measurements made outside of the box, the electrochemical cell was closed with a Teflon cap that had a rubber o-ring to form an airtight seal. Stainless steel rods driven through the cap formed the electrode connections. Cyclic voltammograms (CVs) were obtained on a CH Instruments electrochemical workstation (CHI 660, Austin, TX). Digital simulations of CV were performed using Digisim software (Bioanalytical Systems).

Spectroscopic experiments were done in a 1 cm path length quartz cell. Absorbance spectra were obtained on a Milton Roy spectronic 3000 array spectrophotometer. Fluorescence spectra were collected on a QuantaMaster spectrofluorimeter (Photon Technology International, Birmingham, NJ). The excitation source was a 70 W xenon lamp (LPS-220B Lamp power supply), and the excitation and emission slits were set to 0.5 mm (2 nm bandwidth).

The ECL spectra were obtained on Princeton SPEC-10 Instruments using a charge-coupled device (CCD) camera (Trenton, NJ) cooled to −100 °C with an Acton SpectraPro-150 monochromator (Acton, MA) as the detector. The wavelength scale of the CCD camera and grating system were calibrated using a Hg/Ar pen-ray lamp from Oriel (Stratford, CT). ECL intensity−time curves were collected on an Autolab potentiostat (Ecochemie, Netherlands) connected to a photomultiplier tube (PMT, Hamamatsu, R4220p, Japan). The PMT was supplied with −750 V from a Kepco (New York) high-voltage power supply. The relative ECL intensity was calculated with respect to DPA in 2.33:1 MeCN/PhH by comparison of the maximum intensities in ECL spectra.

Results and Discussion

Electrochemistry. In CV studies, the reversibility, diffusion coefficient, and number of electrons transferred were investigated, as well as the stability of the radical cations and anions of FPhSPFN. A CV showing both reduction and oxidation is

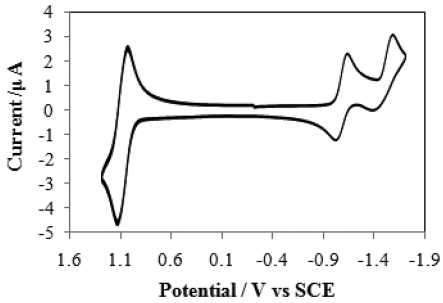

Figure 1. Cyclic voltammogram of 0.5 mM FPhSPFN in 2.33:1 MeCN/PhH with 0.1 M $TBAPF_6$. Scan rate = 100 mV/s. The area of the electrode is 0.019 cm^2.

shown in Figure 1; two reduction waves and one overall oxidation wave were observed. The experimental values obtained for the standard potentials of the reductions are $E^o_{1,red} = -1.09$ V versus SCE and $E^o_{2,red} = -1.50$ V versus SCE. Simulation was done to further investigate the oxidation peak. The results will be shown and discussed later.

The scan rate (v) was changed to study the reversibility of the reduction and oxidation of FPhSPFN. Scan-rate-dependent CVs for the first reduction peak and oxidation are presented in Figure 2. Peak splittings (ΔE_p) for first reduction and oxidation of 0.5 mM FPhSPFN are presented in Table 1. As a reference, ΔE_p for ferrocene performed under the same experimental conditions with different v are also included in Table 1.

From Figure 2, it can be seen that the peak current changed linearly with the square root of the scan rate for both the first reduction ($i_{p,r1}$) and the overall oxidation ($i_{p,o}$), indicating diffusion control of the current. The results in Table 1 show that at small v, the ΔE_p for the first reduction peak is larger than the ~59 mV expected for a Nernstian wave. However, ferrocene, a known Nernstian system studied under the same experimental conditions, shows a similar ΔE_p value. The similarity of peak splitting to ferrocene indicates that the first reduction peak is Nernstian under the experimental conditions and most likely only affected by uncompensated resistance. However, for the oxidation peak, a larger peak splitting than ferrocene is observed; thus, the oxidation is not a single one-electron transfer process and, as shown below, involves a multielectron transfer.

Chronoamperometry at an UME was used to determine the number of electrons, n, exchanged in each electrochemical process observed. The methodology used consists of determining the diffusion coefficient, D, independently from n and with only prior knowledge of the bulk concentration, C^*, and the radius of the UME, a, by normalizing a short time transient with respect to the limiting steady-state current, $i_{d,ss}$.[28] This normalized response is plotted against $t^{-1/2}$, where linear fitting should yield a slope equal to $(2/\pi^{3/2})aD^{-1/2}$. After determining D, n can be calculated based on eq 10 for $i_{d,ss}$

$$i_{d,ss} = 4nFDC^*a \tag{10}$$

where F is Faraday's constant (96 485 C/mol). Before the chronoamperometry study, the linear scan voltammetry of FPhSPFN at a gold UME was studied. The background-subtracted voltammogram is shown in Figure 3. Voltammograms before subtracting the background for FPhSPFN and of the background are shown in Figure S1 (Supporting Information). Two well-separated reduction peaks and a single oxidation peak were observed, consistent with the CV results at a macroelectrode. The value of the steady-state current for oxidation was twice the value of the steady-state current of each reduction wave.

Chronoamperometry results for the first reduction (step potential, $E_{SP} = -1.18$ V versus SCE) and overall oxidation ($E_{SP} = 1.18$ V versus SCE) are shown in Figure 4. In Figure 4, $i(t)/i_{ss}$ are plotted versus $t^{-1/2}$; experimental data show that $i(t)/i_{ss}$ are linearly dependent on $t^{-1/2}$. Linear regression was used to calculate the slope and intercept. The intercepts obtained from all of these cases are very close to 1. The intercept and the linear dependence agree well with the theoretical prediction in a reasonably short time region (≥0.3 s).[28]

The diffusion coefficients and number of electrons calculated from all of the above cases are summarized in Table 2.

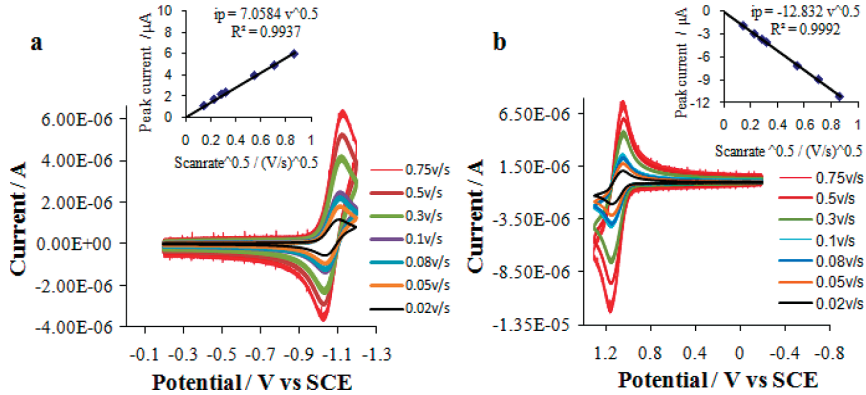

Figure 2. (a) Reduction voltammogram of the first reduction peak of 0.5 mM FPhSPFN in 2.33:1 MeCN/PhH at various v. Inset: First reduction peak current versus $v^{1/2}$. (b) Oxidation CV of 0.5 mM FPhSPFN in 2.33:1 MeCN/PhH at various scan rates. Inset: Oxidation peak current versus $v^{1/2}$.

TABLE 1: Peak Splitting (mV) for the First Reduction Peak and the Overall Oxidation Peak of 0.5 mM FPhSPFN and 1 mM Ferrocene in 2.33:1 MeCN/PhH and 0.1 M $TBAPF_6$ at Various Scan Rates

	0.02 V/s	0.05 V/s	0.08 V/s	0.1 V/s	0.3 V/s	0.5 V/s	0.75 V/s
first reduction	73	77	73	81	87	93	101
overall oxidation	101	102	97	103	109	115	117
ferrocene	73	73	71	75	85	87	95

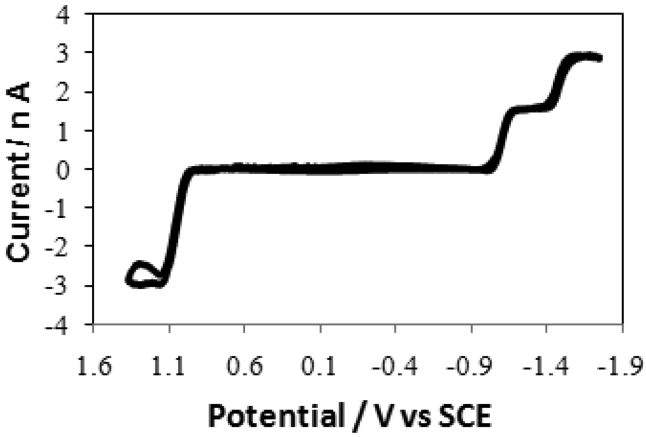

Figure 3. Background-subtracted cyclic voltammogram of 0.5 mM FPhSPFN in 2.33:1 MeCN/PhH and 0.1 M $TBAPF_6$ on gold UME; radius $a = 12.5$ μm. Scan rate = 100 mV/s.

On the basis of the results from chronoamperometry, the reduction involves two one-electron transfer processes, while two electrons are transferred during the oxidation process. These results can be rationalized from the chemical structure of FPhSPFN, which comprises a single fumaronitrile group symmetrically linked through a spirobifluorene group to two triphenylamine groups. Fumaronitrile is a good electron acceptor, and triphenylamine is a good electron donor. The two reduction peaks are thus assigned to the stepwise reduction of the fumaronitrile moiety to form the radical anion $A^{-\bullet}$; then, reduction to $A^{2-\bullet}$ occurs, as observed in the absence of water.[29] The electron-donating triphenylamine moieties are separated by two spirobifluorene moieties and one fumaronitrile moiety; therefore, the two oxidation centers are far apart and not well-conjugated. Thus, in the case of oxidation, the loss of an electron from one triphenylamine group to form the radical cation does not greatly influence the oxidation of the second triphenylamine group, so that a single two-electron wave is observed for the oxidation. This observation is consistent with similar cases in which two unconjugated 9,10-diphenylanthracence groups separated by a spirobifluorene linker show a single oxidation peak.[20] Furthermore, if the two triphenylamine groups are separated by a shorter, conjugated linker, they do show the appearance of two one-electron waves.[21] In the experiment, no spirobifluorene redox peaks were observed within the potential window of the solvent used. This also occurs when other more easily oxidizable groups are attached to this moiety; the direct reduction of unsubstituted spirobiflourene has been shown to be as negative as −2.85 V versus SCE, and its oxidation has been shown to yield an irreversible voltammogram at 1.54 V versus SCE.[21]

TABLE 2: *D* and *n* Values for the First Reduction and Overall Oxidation of 0.5 mM FPhSPFN in 0.1M $TBAPF_6$[a]

reaction	i_{ss}/nA	10^6 D/cm^2 s^{-1}	n
first reduction	1.33	5.34	1.04
overall oxidation	2.5	5.41	1.79

[a] Solvent: 2.33:1 MeCN/PhH. Electrode radius: $a = 12.5$ μm.

CV Simulation. Digital simulations of the experimental CVs of the oxidation shown in Figure 5 were carried out to obtain a better estimate of the degree of splitting of the oxidation wave. The double layer capacitance was calculated to be 0.8 μF (42.1 μF/cm^2), and the uncompensated resistance was 1000 Ω (see Figure S2 in the Supporting Information). The CV simulation mechanism assigned two reversible, one-electron processes for the oxidation with the ΔE^o between the two waves to be 63 mV and $D = 8.75 \times 10^{-6}$ cm^2/s, $E^o_{1,ox} = 1.05$ V versus SCE, and $E^o_{2,ox} = 1.11$ V versus SCE. The plots in Figure 5 indicate good fits between experimental and simulated oxidation CVs performed at various scan rates from 0.05 to 0.75 V/s.

Spectroscopy. The same solvent was used for the spectroscopic as that for the electrochemical measurements. The absorption spectrum in Figure 6 shows absorption maxima at 310 and 456 nm. The absorption at 310 nm is close to that observed for the spirobifluorene group.[26] The molar extinction coefficient calculated at 310 nm is 4.59×10^4 M^{-1} cm^{-1}, and that at 456 nm is 2.65×10^4 M^{-1} cm^{-1}.

The photoluminescence with excitation at 456 nm, also shown in Figure 6, produces an emission maximum at 673 nm. The large Stokes shift of 217 nm is consistent with significant structural rearrangement and a large dipole moment change upon excitation and emission of FPhSPFN.[30]

The energy of the excited singlet state is calculated based on the equation E_s (in eV) = 1239.81/λ (in nm),[1] where λ is the wavelength at maximum PL emission. The calculated excited singlet state energy is 1.83 eV. The energy of the annihilation reaction, $-\Delta H^o = E^o_{ox} - E^o_{red} - T\Delta S$, based on the difference between the thermodynamic potentials of the overall oxidation and the first reduction waves in the cyclic voltammogram ($E^o_{ox} - E^o_{red} = 2.17$ eV) with an estimated entropy effect (∼0.1 eV) subtracted out, is about 2.07 eV. The energy of the annihilation reaction (2.07 eV) is greater than the energy needed to directly populate the singlet excited state (1.83 eV); thus, the singlet excited states can be directly populated upon radical ion annihilation.[1] It has been suggested that in systems with large Stokes shifts, a more correct calculation of the energy of the excited singlet state energy can be estimated by considering the wavelength where the absorbance and emission curves cross;[1] in our case, this would yield an excited singlet state energy of 2.33 eV (at 531 nm), for which our estimated $-\Delta H^o = 2.07$ eV would

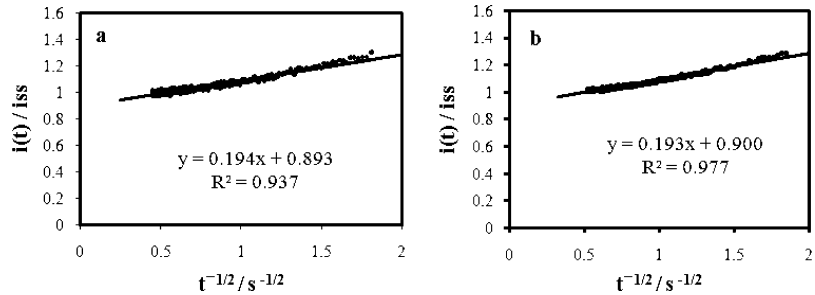

Figure 4. Plot of the experimental ratio $i_d(t)/i_{d,ss}$ against the inverse square root of time of 0.5 mM FPhSPFN in 0.1 M $TBAPF_6$ with a 12.5 μm radius Au UME in 2.33:1 MeCN/PhH. (a) First reduction at a step potential of $E_{SP} = -1.18$ V versus SCE. (b) Overall oxidation at $E_{SP} = 1.18$ V versus SCE.

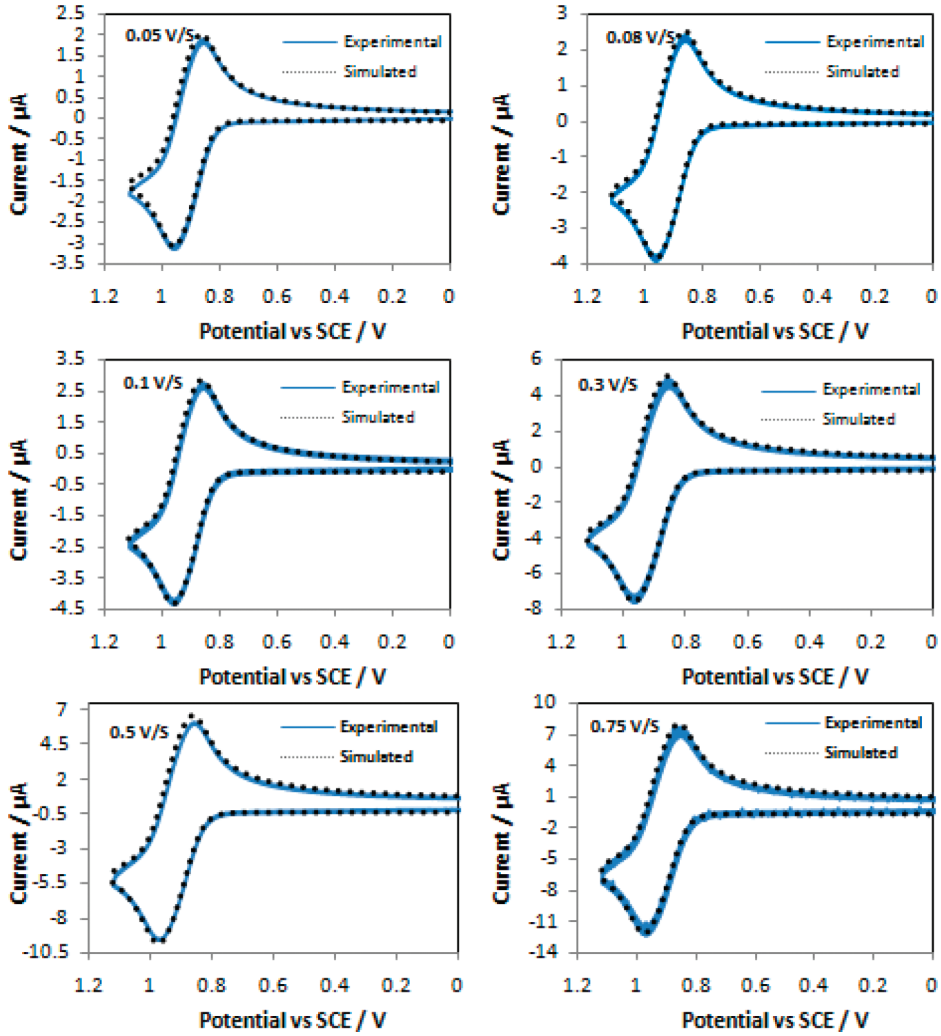

Figure 5. Simulation of 0.5 mM $FPhSPF_6$ oxidation at (a) 0.05, (b) 0.08, (c) 0.1, (d) 0.3, (e) 0.5, and (f) 0.75 V/s. The simulation mechanism is two one-electron oxidations with $D = 8.75 \times 10^{-6}$ cm^2/s, $E^o_{1,ox} = 1.05$ V versus SCE, $E^o_{2,ox} = 1.11$ V versus SCE, $k^o = 10^4$ cm/s, $\alpha = 0.5$, uncompensated solution resistance $R_u = 1000\ \Omega$, and double layer capacitance $C_{dl} = 0.8\ \mu$F.

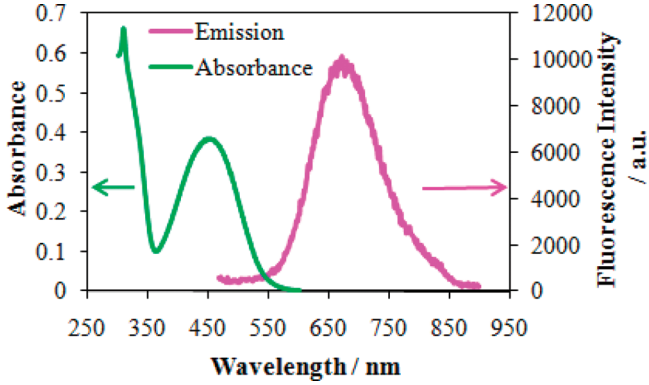

Figure 6. Absorbance and fluorescence emission spectra of a solution of 14.5 μM FPhSPFN in 2.33:1 MeCN/PhH (excitation wavelength, 456 nm).

be insufficient to populate it. Experimentally, we observe that upon pulsing into the second reduction process (Figure 11), where $-\Delta H^o = 2.48$ eV and the calculated singlet state energy is higher, the ECL emission profile is maintained, suggesting that in this excess energy scenario, the same excited state is formed and is thus energy-sufficient even for the first reduction-complete oxidation case. Given the uncertainties presented by each calculation method, we assign it to an energy-sufficient system by considering the maximum of the PL emission, as is usually done for ECL systems.[10]

ECL Spectrum: Solvent Dependence and Coreactant ECL. Figure 7a shows the ECL spectrum obtained by pulsing between reduction and oxidation potentials that gave similar electrochemical currents in order to have an approximate stoichiometry of 1:1 radical anions with radical cations (80 mV past the first reduction peak and at the half-wave oxidation potential, respectively) and the photoluminescence spectrum, both for the solvent composition of 2.33:1 MeCN/PhH.

A red shift of 35 nm was observed for ECL as compared with PL. Note that because of the large Stokes shift, FPhSPFN shows very little absorbance within the wavelength range of PL and ECL (Figure 6); therefore, although the concentration of FPhSPFN is much smaller in the PL experiment, absorption of the emitted light in ECL is not significant. We have also carried out ECL experiments with similar concentrations of FPhSPFN as those used in PL (e.g., 20 μM), and the normalized ECL spectra show the same shape and location as in the more concentrated cases with the same peak shift. These results suggest that the red shift of the ECL spectra is not due to self-absorbance or an inner filter effect as is often seen in ECL when compared to PL. There is also the possibility that systematic errors in the spectroscopy can account for some of the difference since the PL and ECL spectra were taken with different

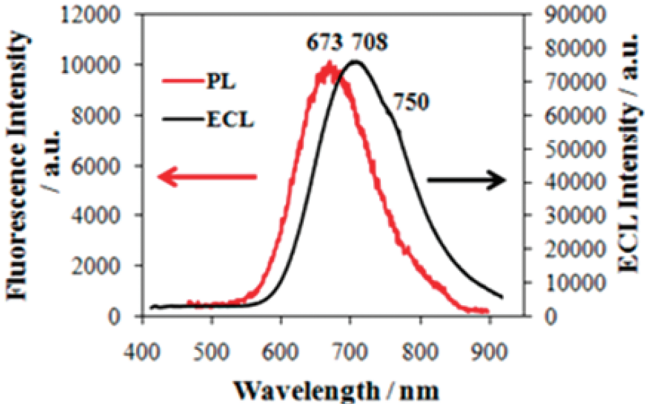

Figure 7. Fluorescence or photoluminescence (PL) spectra of 14.5 μM FPhSPFN in 2.33:1 MeCN/PhH and ECL spectra of 0.5 mM FPhSPFN in 0.1 M $TBAPF_6$ in 2.33:1 MeCN/PhH with pulsing between +1.02 and −1.18 V (versus SCE) (half oxidation and 80 mV past the first reduction peak potential). ECL spectra were integrated for 1 min using a 1 mm slit width. (Excitation wavelength for fluorescence emission: 456 nm).

instruments. However, our extensive experience with these measurements in previous ECL studies indicates that this would result, at most, in a shift of 10−15 nm. Figure 7 reveals a shoulder near 750 nm clearly seen for ECL. In order to understand better the origin of this shoulder, both ECL and PL experiments were done in solvents with different ratios of benzene (PhH) to acetonitrile (MeCN) to change the polarity of the solvent medium without compromising our ability to carry out electrochemical measurements (because of increasing solution resistance with addition of PhH). The results of PL with various MeCN/PhH ratios are shown on absolute and normalized scales in Figure 8a and b, respectively. In general, the system shows solvatochromism, with increasing fluorescence intensity and a blue shift in the peak wavelength with decreasing solvent polarity (increase in the fraction of benzene). This strongly suggests that the excited state has a high dipole moment; thus, it is less stabilized by a nonpolar solvent such as benzene, yielding a shorter radiative lifetime of the excited state (which results in faster radiative decay that is less prone to quenching or radiationless decay) and a smaller Stokes shift.[31,32] Figure 8b also reveals that the PL spectra broaden and show the growth of a very low intensity shoulder between 750 and 850 nm with increasing solvent polarity (~30% of the main peak height when larger fractions of acetonitrile were used).

Correspondingly, the ECL spectra with different PhH to MeCN ratios are presented in Figure 9a and b, on an absolute scale and normalized scales. The same trend was observed as in PL; peak intensities increased and peak wavelengths blue-shifted as the solvent polarity decreased. Thus, there is some correlation between the behavior of PL and ECL, suggesting that similar excited states are involved. The normalized ECL spectra (Figure 9b) show more clearly that the shoulder at around 750 nm relatively increased in intensity with increasing solvent polarity.

Further ECL experiments were carried out to test possibilities for the origin of this shoulder, such as the formation of excimers. When the ECL spectrum is obtained by the use of a correactant, such as BPO as shown in Figure 10, the shoulder is still present in the same proportions as in the annihilation case; while this is not strictly conclusive, it does suggest strongly that the formation of an excimer is not the reason for the observation of the shoulder.

A mechanistic note worth considering in the case of FPhSPFN is that the presence of two oxidizable and two reducible moieties may lead to unusual charged excited states by virtue of the annihilation of multiply charged species, for example, a dication with an anion radical. As can be seen in the Supporting Information, Figure S3, the normalized ECL spectra for the comparison of the annihilation reactions of the dication−anion

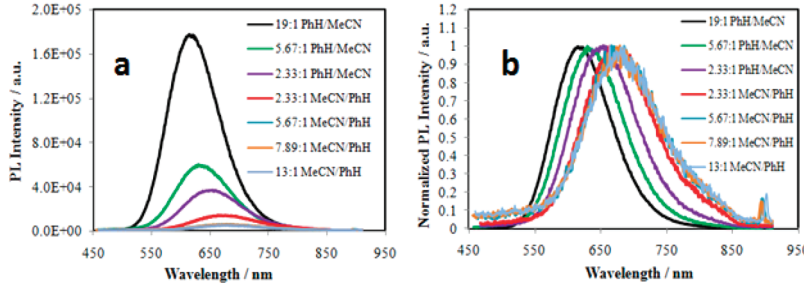

Figure 8. Fluorescence spectra of 14.5 μM FPhSPFN in solvents of different MeCN/PhH ratios. (a) Before normalization. (b) After normalization.

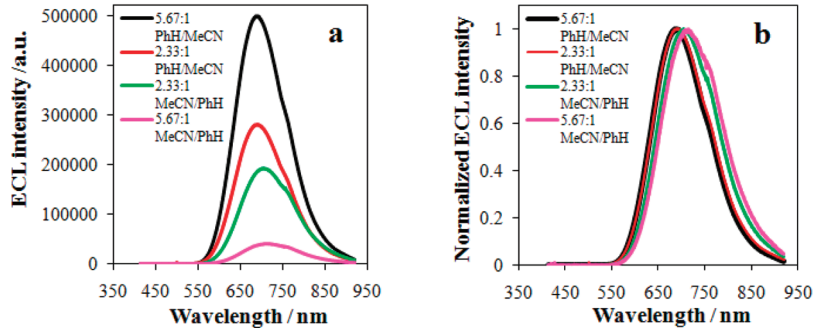

Figure 9. ECL spectra of 0.5 mM FPhSPFN in solvents of different MeCN/PhH ratios with pulsing between +1.18 and −1.18 V (versus SCE) (80 mV over the whole oxidation and first reduction peak potentials). (a) Before normalization. (b) After normalization. ECL spectra were integrated for 1 min using a 1 mm slit width. Supporting electrolyte: 0.1 M $TBAPF_6$. Electrode area: 0.028 cm^2. In the case of 5.67:1 MeCN/PhH, 0.25 mM FPhSPFN was used because of its limited solubility.

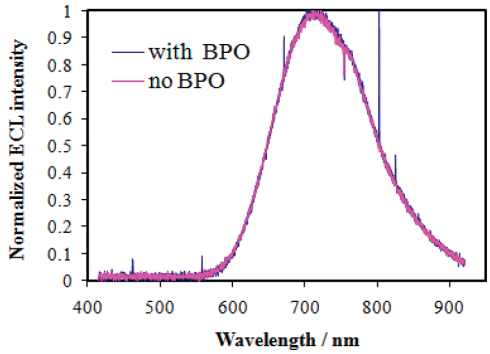

Figure 10. Normalized ECL spectra of FPhSPFN with the presence of BPO coreactant and without BPO coreactant in 13:1 MeCN/PhH when pulsing between +1.18 and −1.18 V (versus SCE) (80 mV over the whole oxidation and first reduction peak potentials). ECL spectra were integrated for 1 min using a 1 mm slit width.

TABLE 3: Maximum ECL Emission Wavelength λ_{max}^{ECL}, Intensity at λ_{max}^{ECL}, and Relative Intensity with Respect to DPA

solvent	λ_{max}^{ECL} (nm)	$I_{\lambda max}^{ECL}$ (au)	relative intensity wrt DPA[a]
PhH/MeCN 5.67:1	687	5.0×10^5	16%
PhH/MeCN 2.33:1	690	2.8×10^5	8.7%
MeCN/PhH 2.33:1	708	1.9×10^5	6%

[a] Calculated by comparing the $I_{\lambda max}^{ECL}$ of FPhSPFN with that of DPA in MeCN/PhH 2.33:1.

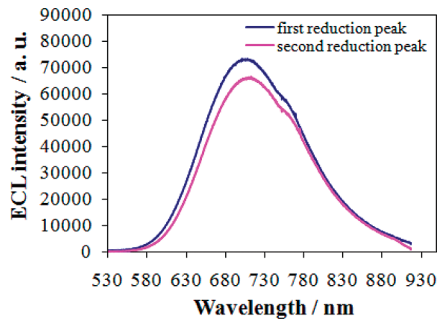

Figure 11. ECL spectra of 0.5 mM FPhSPFN in 0.1 M $TBAPF_6$ in 2.33:1 MeCN/PhH obtained by pulsing between +1.02 V versus SCE and two different cathodic potentials (−1.18 V versus SCE and −1.638 V versus SCE). ECL spectra were integrated for 1 min using a 1 mm slit width.

and cation−anion pairs (produced by judicious choice of the oxidation stepping potential) are essentially the same. One other possibility for the origin of this peak may lie in the formation of an internal charge-transfer state, as has been suggested with certain ECL systems;[33,34] however, the broadness of the overall emission and the degree of overlapping with the main emission prevent us from drawing further conclusions in this case.

On the basis of the results of Figure 9a, a comparison of the relative ECL intensity of 0.5 mM FPhSPFN in different solvents with respect to 0.5 mM DPA is shown in Table 3.

A comparison of the ECL spectra collected with the first reduction and second reduction is shown in Figure 11. A potential excursion into the second reduction process to generate the radical dianion showed a decrease in the ECL intensity. We believe that a following chemical process consumes in part the radical dianion, as evidenced by the lack of reversibility observed in the CV when going into the second reduction peak. The observed formation of a film on the electrode when stepping into such reduction potentials may also play a role in this ECL intensity decrease.

Transient ECL. Observation of the ECL transients during potential pulsing with different pulse durations can provide information about the ECL process and reactant stability.[35] For example, when the radical ions are generated under mass-transfer-controlled conditions and are stable during a pulse, the ECL emission pulses are of equal height and constant with pulsing. Instability of one of the radical ion species results in unequal heights for the anodic and cathodic pulses and a decay of the ECL emission with time.

During the reduction and oxidation of FPhSPFN, four kinds of radical ions can be formed, the dianion ($D-X-A^{2-\bullet}-X-D$), the radical anion ($D-X-A^{-\bullet}-X-D$), the dication ($D^{+\bullet}-X-A-X-D^{+\bullet}$), and the radical cation ($D^{+\bullet}-X-A-X-D$). We investigated what combinations of these species produce stable and intense ECL. For this purpose, we observed the ECL transients with a PMT while pulsing between certain combinations of potentials for oxidation and reduction. Figure 12 shows the results of this technique for the relevant combinations of generated species. Figure 12a, in which approximately the same amounts of anion and cation radicals are produced in each pulse, shows that the ECL response is fairly symmetrical, but with a slightly lower ECL intensity in the anodic pulse. Often, this behavior suggests instability of the formed radical anions; however, no indication of this type of effect is provided in the well-behaved electrochemistry already described for FPhSPFN. The electrochemical control of the stoichiometry of the annihilation reaction in the case presented in Figure 12a is more difficult than that in the simpler case where only the radical anion and cation are generated as there is always uncertainty about how much of the radical dication is being produced concurrently with the radical cation (either by direct generation or by disproportionation of the radical cations). Figure 12b shows the more controllable production of an excess of radical cation equivalents upon anodic stepping into the overall oxidation wave. It was observed that in this situation, a more long-lasting ECL signal was obtained, as evidenced in Figure 12b during the cathodic pulse. Integration of the transients in Figure 12a and b for one cycle, that is, an oxidation and a reduction step, showed a four-fold increase in the ECL intensity when stepping into the whole oxidation wave compared to the case of only half of the oxidation wave. Finally, Figure 12c shows that upon stepping to the second reduction wave, the emission observed in the anodic pulses is greatly reduced, thus confirming the instability of the dianion, which is consistent with the shape of the second reduction wave in the cyclic voltammetry and the decrease in the intensity of the ECL response shown in Figure 11 when stepped into the second reduction wave. Comparison of the ECL transients presented in this section to the ones obtained under ideal conditions through digital simulation is found in the Supporting Information, Figures S4 to S6.

Conclusions

We report here the electrochemistry and ECL of a novel red-emitting OLED compound, the donor−linker−acceptor−linker−donor molecule FPhSPFN. The presence of a fumaronitrile moiety as the electron acceptor and a triphenylamine moiety as the electron donors allows the generation of ECL without the addition of a coreactant or a second compound. The nonplanar bulky spirobifluorene linker prevents the delocalization of charges through the whole molecule and favors the localization of the negative charge of the radical anions on the

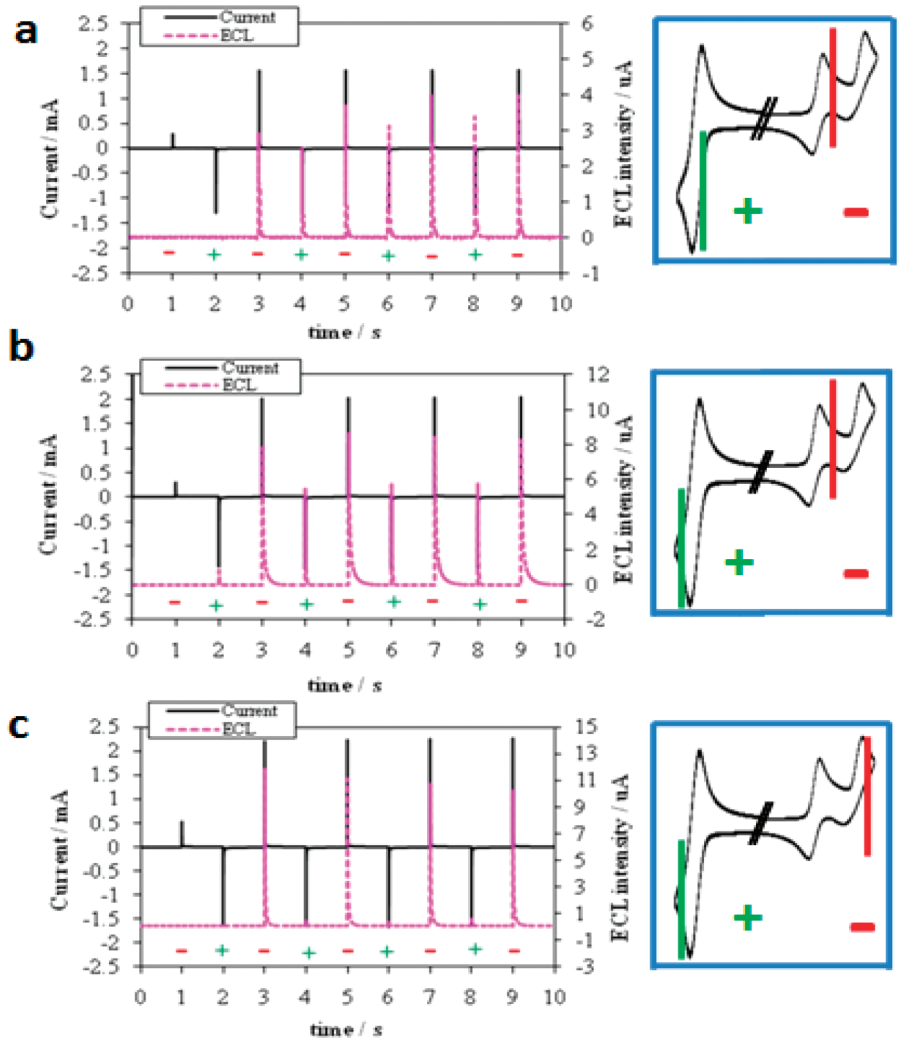

Figure 12. Current (black, solid) and ECL (pink, dotted) transients with 1 s of pulsing time for 0.5 mM FPhSPFN in 2.33:1 MeCN/PhH pulsed between (a) first reduction and half oxidation, (b) first reduction and whole oxidation, and (c) second reduction and whole oxidation. Panels on the right show schematically the potentials used and the polarity of the step as indicated in the graphs.

fumaronitrile group and of the positive charge of the radical cations on each triphenylamino group. The wavelengths and intensities of ECL and PL vary significantly with solvent polarity, indicative of the formation of emissive excited states having high dipole moments. The instability of the dianion gives rise to low ECL intensity upon radical ion annihilation. The energy of this annihilation reaction is sufficiently high to generate the singlet excited state and the corresponding ECL emission. The compound shows an increase of ECL intensity with decreasing solvent polarity and has a relative ECL intensity between 6 and 16% of DPA. The results demonstrate the possibility of designing donor−acceptor-based molecules for efficient ECL.

Acknowledgment. We thank Khalid M. Omer and Matthew M. Sartin for technical assistance, Alec Nepomnyashchii and Cunzhong Zhang for helpful discussions, and the financial support of The National Science Foundation (CHE 0808927), Academia Sinica, and the National Science Council of Taiwan. J.R.-L. thanks Eli Lilly and Company for an ACS Division of Analytical Chemistry fellowship, as well as Secretaria de Educacion Publica of Mexico and the Mexican Government for scholarship support.

Supporting Information Available: CVs on UME without background subtraction and background (Figure S1), calculation of double layer capacitance (C_{dl}) (includes Table 1 and Figure S2), spectral features observed for the ECL of FPhSPFN, and the procedure used for digital simulation of the ECL transients as well as Figures S4−S6. This material is available free of charge via the Internet at http://pubs.acs.org.

References and Notes

(1) Bard, A. J. In *Electrogenerated Chemiluminescence*; Bard, A. J., Ed.; Marcel Dekker: New York, 2004.

(2) For reviews on ECL, see: (a) Richter, M. M. *Chem. Rev.* **2004**, *104*, 3003–3036. (b) Knight, A. W.; Greenway, G. M. *Analyst* **1994**, *119*, 879–890. (c) Faulkner, L. R.; Bard, A. J. *Electroanalytical Chemistry*; Marcel Dekker: New York, 1977; Vol. 10, p 1. (d) Bard, A. J.; Debad, J. D.; Leland, J. K.; Sigal, G. B.; Wilbur, J. L.; Wohlstadter, J. N. In *Encyclopedia of Analytical Chemistry: Applications, Theory and Instrumentation*; Meyers, R. A., Ed.; John Wiley & Sons: New York, 2000; Vol. 11, p 9842.

(3) Forry, S. P.; Wightman, R. M. In *Electrogenerated Chemiluminescence*; Bard, A. J., Ed.; Marcel Dekker: New York, 2004; p 277.

(4) Maloy, J. T. In *Electrogenerated Chemiluminescence*; Bard, A. J., Ed.; Marcel Dekker: New York, 2004; p 159.

(5) Keszthelyi, C. P.; Tokel-Takvoryan, N. E.; Bard, A. *J. Anal. Chem.* **1975**, *47*, 249–256.

(6) Kapturkiewicz, A. *J. Electroanal. Chem.* **1994**, *372*, 101–116.

(7) Sartin, M. M.; Zhang, H. Y.; Zhang, J. Y.; Zhang, P.; Tian, W. J.; Wang, Y.; Bard, A. J. *J. Phys. Chem. C* **2007**, *111*, 16345–16350.

(8) Choi, J.-P.; Wong, K.-T.; Chen, Y.-M.; Yu, J.-K.; Chou, P.-T.; Bard, A. J. *J. Phys. Chem. B.* **2003**, *107*, 14407–14413.

(9) Lai, R. Y.; Kong, X. X.; Jenekhe, S. A.; Bard, A. J. *J. Am. Chem. Soc.* **2003**, *125*, 12631–12639.

(10) Lai, R. Y.; Fabrizio, E. F.; Lu, L.; Jenekhe, S. A.; Bard, A. J. *J. Am. Chem. Soc.* **2001**, *123*, 9112–9118.

(11) Izadyar, A.; Omer, K. M.; Liu, Y. Q.; Chen, S. Y.; Xu, X. J.; Bard, A. J. *J. Phys. Chem. C* **2008**, *112*, 20027–20032.

(12) Fungo, F.; Wong, K.-T.; Ku, S.-Y.; Hung, Y.-Y.; Bard, A. J. *J. Phys. Chem. B* **2005**, *109*, 3984–3989.

(13) Richter, M. M. In *Electrogenerated Chemiluminescence*; Bard, A. J., Ed.; Marcel Dekker: New York, 2004; p 306.

(14) Tokel, N.; Bard, A. J. *J. Am. Chem. Soc.* **1972**, *94*, 2862–2863.

(15) Juris, A.; Balzani, V.; Barigelletti, F.; Campagna, S.; Belser, P.; Von Zelewsky, A. *Coord. Chem. Rev.* **1988**, *84*, 85–277.

(16) Pan, Y.; Zhao, J. S.; Ji, Y. Y.; Yan, L.; Yu, S. Q. *Chem. Phys.* **2006**, *320*, 125–132.

(17) Chiu, K. Y.; Su, T. X.; Li, J. H.; Lin, T.-H.; Liou, G.-S.; Cheng, S.-H. *J. Electroanal. Chem.* **2005**, *575*, 95–101.

(18) Zou, Y. P.; Sang, G. Y.; Wan, M. X.; Tan, S. T.; Li, Y. F. *Macromol. Chem. Phys.* **2008**, *209*, 1454–1462.

(19) Hancock, J. M.; Gifford, A. P.; Zhu, Y.; Lou, Y.; Jenekhe, S. A. *Chem. Mater.* **2006**, *18*, 4924–4932.

(20) Sartin, M. M.; Shu, C. F.; Bard, A. J. *J. Am. Chem. Soc.* **2008**, *130*, 5354–5360.

(21) Fungo, F.; Wong, K.-T.; Ku, S.-Y.; Hung, Y.-Y.; Bard, A. J. *J. Phys. Chem. B* **2005**, *109*, 3984–3989.

(22) Natera, J.; Otero, L.; D'Eramo, F.; Sereno, L.; Fungo, F.; Wang, N.-S.; Tsai, Y.-M.; Wong, K.-T. *Macromolecules* **2009**, *42*, 626–635.

(23) Ho, T.-I.; Elangovan, A.; Hsu, H.-Y.; Yang, S.-W. *J. Phys. Chem. B* **2005**, *109*, 8626–8633.

(24) Mitschke, U.; Bäuerle, P. *J. Mater. Chem.* **2000**, *10*, 1471–1507.

(25) Gross, E. M.; Anderson, J. D.; Slaterbeck, A. F.; Thayumanavan, S.; Barlow, S.; Zhang, Y.; Marder, S. R.; Hall, H. K.; Flore Nabor, M.; Wang, J.-F.; Mash, E. A.; Armstrong, N. R.; Wightman, R. M. *J. Am. Chem. Soc.* **2000**, *122*, 4972–4979.

(26) Rashidnadimi, S.; Hung, T. H.; Wong, K.-T.; Bard, A. J. *J. Am. Chem. Soc.* **2008**, *130*, 634–639.

(27) Lee, Y.-T.; Chiang, C.-L.; Chen, C.-T. *Chem. Commun.* **2008**, 217–219.

(28) Denuault, G.; Mirkin, M. V.; Bard, A. J. *J. Electroanal. Chem.* **1991**, *308*, 27–38.

(29) Grimshaw, J. *Electrochemical Reactions and Mechanisms in Organic Chemistry*; Elsevier: Amsterdam, The Netherlands, 2000; p 66.

(30) Berlman, I. B. *Handbook of Fluorescence Spectra of Aromatic Molecules*, 2nd ed.; Academic Press: New York, 1971.

(31) Lakowicz, J. R. *Principles of Fluorescence Spectroscopy*, 3rd ed; Springer Science + Business Media: New York, 2006.

(32) Nigam, S.; Rutan, S. *Appl. Spectrosc.* **2001**, *55*, 362A–370A.

(33) Kapturkiewicz, A.; Herbich, J.; Nowacki, J. *Chem. Phys. Lett.* **1997**, *275*, 355–362.

(34) Itaya, K.; Toshima, S. *Chem. Phys. Lett.* **1977**, *51*, 447–452.

(35) (a) Ref 1, Chapters 2 (Fan, F.-R. F.) and 3 (Maloy, J. T.); (b) Cruser, S. A.; Bard, A. J. *J. Am. Chem. Soc.* **1969**, *91*, 267.

JP911451V